

**SMR.1580 - 23**

**CONFERENCE ON FUNDAMENTAL SYMMETRIES  
AND FUNDAMENTAL CONSTANTS**

**15 - 18 September 2004**

**UNIVERSAL DYNAMICS OF SPONTANEOUS LORENTZ  
VIOLATION AND A NEW SPIN-DEPENDENT  
INVERSE-SQUARE LAW FORCE**

**J. Thaler  
Harvard U., USA**

# Universal Dynamics of Spontaneous Lorentz-Violation and a New Spin-Dependent Inverse-Square Law Force

Nima Arkani-Hamed, Hsin-Chia Cheng, and Jesse Thaler

May 999, 2004

## **Abstract**

Yada, yada, yada.

## 1 Introduction

The theory of ghost condensation [1] is the universal low-energy effective theory coming from spontaneous time diffeomorphism breaking. While the theory can be derived by considering the stabilization of a scalar field with wrong-sign kinetic terms, the low energy effective Lagrangian is appropriate for *any* theory that is rotationally invariant but exhibits spontaneous Lorentz symmetry breaking. In particular, ghost condensation describes the Higgs phase of gravity, whether or not a ghost field actually triggered the spontaneous symmetry breaking. This is the exact analog of the Higgs mechanism in gauge theories; the language of tachyon condensation is a convenient way to conceptualize spontaneous gauge symmetry breaking, but the actual universal low-energy description involves the Goldstone bosons associated with the broken symmetry directions.

Most work on ghost condensation has focused on gravitational phenomena. The Goldstone boson associated with broken time diffeomorphisms — hereafter dubbed the ghostone boson — mixes with gravity in an interesting way, leading to modifications of Newton’s law at large distances and late times. However, the modifications to the gravitational potential are strongly suppressed when the sources are moving with some velocity with respect to the preferred rest frame of the ghostone [3, 4]. Recent, it has been realized that even for moderately sized gravitational sources such as the earth, the classical equation of motion for the ghostone boson is quickly dominated by non-linear terms, so a complete understanding of the infrared modifications to gravity will have to account for these non-linear effects [ref?]. Also, the ghostone boson has been incorporated into a candidate theory for inflation that exhibits different experimental signatures from the standard slow-roll scenario [2].

But the ghostone boson is not just interesting for its cosmological consequences. Because ghost condensation can describe Lorentz-violations in a completely consistent framework, it is ideally suited to understand possible Lorentz- and CPT-violations in the Standard Model. Most of the previous work in this area has focused on cataloging all Lorentz-violating spurious coupling constants [ref?], leaving the origin of these spurions as an open question. Experiments in a wide variety of physical systems have placed considerable bounds on these couplings [ref?]. Now using the language of ghost condensation, we will see that every spurion actually comes paired with a coupling to the ghostone boson. This will lead to novel Lorentz-violating *dynamics*, opening up new avenues to explore possible violations of the fundamental symmetries of the Standard Model.

In this paper, we will focus on the coupling between the ghostone boson and fermion axial currents (known as spin densities in the non-relativistic limit). Though these couplings can be forbidden by a discrete symmetry, they are the leading couplings to the Standard Model and therefore the most dangerous (and interesting) phenomenologically. The analysis in this paper will naturally carry over to similar couplings that are guaranteed to show up at least at the level of graviton loops.

We will explore two dynamical effects that both capitalize on the fact the ghostone boson has an unusual Lorentz-violating  $\omega \sim k^2/M$  dispersion relation. The first effect is the analog of Cherenkov radiation, where spin sources radiate away kinetic energy until they are at rest relative to the ghostone rest frame. The second effect is a long-range  $1/r$  spin-dependent potential that exhibits an interesting velocity dependence. It is worth emphasizing that these novel dynamical effects are indeed phenomenological viable, and while constraints on Lorentz-violating spurions place bounds on the couplings to the ghostone boson, there are still regions of parameter space that are not excluded and which may be accessible in future

experiments.

Also, it is amusing to note that the theory of ghost condensation is really the effective field theory of the ether, in the sense that it is a consistent way to identify a preferred cosmological rest frame. Unlike the luminous ether, which was a inelegant solution to a nonexistent problem, the ghostone boson has the physical interpretation of characterizing the extent of local Lorentz violations at low energies. Though we will resist the temptation to call the ghostone boson an “etheron”, we will use the terms “ether rest frame” and “ether wind” as mnemonics.

We start with a review of the Goldstone boson language of spontaneous time diffeomorphism breaking and show how to generate all allowed couplings to the ghostone boson. We briefly comment on possible modifications to this story coming from non-linear effects on the gravitational side of the theory as well as bounds from astrophysics. We then focus on the coupling to fermion axial currents, and elaborate on ghostone Cherenkov radiation and the new spin-dependent force. In the last section, we summarize existing constraints on the parameters of the theory and comment on future work.

## 2 Preliminaries

### 2.1 Review of Spontaneous Time Diffeomorphism Breaking

In the original language of ghost condensation, the theory is described by a scalar picking up a time-dependent vacuum expectation value  $\langle\phi\rangle = M^2 t$ . The excitation around this vacuum is the ghostone boson  $\pi$ , and in the limit that gravity decouples from the ghostone boson sector, the kinetic terms for  $\pi$  are

$$\mathcal{L} = \frac{1}{2}\dot{\pi}^2 - \frac{1}{2M}(\nabla^2\pi)^2, \quad (1)$$

where dots indicate time derivatives, gradients refer to spatial gradients, and  $M$  is the scale of spontaneous time diffeomorphism breaking. We immediately see the Lorentz-violating  $\omega \sim k^2/M$  dispersion relation for the ghostone boson. As shown in [1], the reason there is not the standard  $(\nabla\pi)^2$  spacial kinetic piece is that it is forbidden by residual spacial diffeomorphisms.

It is straightforward to couple matter to the ghostone boson. The scalar  $\phi$  has a shift symmetry  $\phi \rightarrow \phi + c$ , so all allowed interactions between the ghostone boson and Standard Model fields can be generated by writing down all Lorentz-invariant combinations involving  $\partial_\mu\phi$  and then expanding about the  $\phi$  vev. For example, from the term  $\bar{\Psi}\gamma^\mu\gamma^5\Psi\partial_\mu\phi/F$ , we generate the interaction which will play a major role in our analysis:

$$\mathcal{L}_{\text{int}} = \frac{1}{F} (M^2\bar{\Psi}\gamma^0\gamma^5\Psi + \bar{\Psi}\gamma^\mu\gamma^5\Psi\partial_\mu\pi). \quad (2)$$

While this construction is convenient, it masks a key point. The above interaction is certainly Lorentz- and CPT-violating, but it is not clear why the first term (which modifies the dispersion relation for the fermion) is paired with a seemingly Lorentz-invariant coupling to the ghostone boson.

The reason is again residual spacial diffeomorphisms, and this is easiest to see in the language of Goldstone bosons. If we expand the metric about flat space,  $g_{\mu\nu} = \eta_{\mu\nu} + h_{\mu\nu}$ , then to leading order the

space-time diffeomorphism generated by  $x^\mu \rightarrow x^\mu + \xi^\mu(x)$  is

$$h_{\mu\nu} \rightarrow h_{\mu\nu} - \partial_\mu \xi_\nu - \partial_\nu \xi_\mu + \dots, \quad (3)$$

where there are additional terms at  $\mathcal{O}(\xi^2)$  and  $\mathcal{O}(h\xi)$ . To this order, a vector field  $J_\mu$  transforms under the diffeomorphism as

$$J_\mu \rightarrow J_\mu - (\partial_\mu \xi^\nu) J_\nu - \xi^\nu \partial_\nu J_\mu. \quad (4)$$

If we now consider the leading order couplings between  $J_\mu$  and  $h_{\mu\nu}$  that break  $\xi^0$  but preserve  $\xi^i$  and  $SO(3)$  rotations, we find

$$\mathcal{L}_{\text{int}} = \alpha \left( J_0 + h_{0i} J_i - \frac{1}{2} h_{ii} J_0 \right) + \alpha' h_{00} J_0, \quad (5)$$

where  $\alpha$  and  $\alpha'$  are arbitrary constants and a sum over  $i$  is implied. Note that the terms in parenthesis are *forced* to have a shared coupling constant because of the  $\xi^i$  diffeomorphisms.

To see what equation (5) looks like in terms of Goldstone bosons, we can simply perform the broken  $\xi^0$  diffeomorphism and promote  $\xi^0$  to the ghostone field  $\pi$ . Because the kinetic term for  $\pi$  is healthy in the limit that gravity decouples, we can safely consider the interactions when  $M_{\text{Pl}} \rightarrow \infty$  (equivalently, when  $h_{\mu\nu} = 0$ ). After going to canonical normalization for the ghostone boson ( $\pi \rightarrow \pi/M^2$ ) we are left with the interaction

$$\mathcal{L}_{\text{int}} = \frac{1}{F^{s-2}} \left( M^2 J_0 - \vec{J} \cdot \vec{\nabla} \pi \right) + \frac{1}{F'^{s-2}} (J_0 \dot{\pi}), \quad (6)$$

where  $F$  and  $F'$  are independent mass scales and  $s$  is the mass dimension of  $J_\mu$ . Note that in equation (2), we have only recovered the interaction with the choice  $F = F'$ . In the original ghost language, we can see that  $F$  and  $F'$  are indeed independent by expanding interactions of the form

$$J^\mu \partial_\mu \phi \left( \frac{\partial^\nu \phi \partial_\nu \phi}{M^4} \right)^n \rightarrow \left( M^2 J_0 - \vec{J} \cdot \vec{\nabla} \pi \right) + (2n+1) J_0 \dot{\pi}. \quad (7)$$

We can repeat the above procedure to find the couplings of a scalar  $\chi$  or a symmetric tensor  $T_{\mu\nu}$  to the ghostone boson. Under the full diffeomorphisms

$$\begin{aligned} \chi &\rightarrow \chi - \xi^\mu \partial_\mu \chi, \\ T_{\mu\nu} &\rightarrow T_{\mu\nu} - \partial_\mu \xi^\rho T_{\rho\nu} - \partial_\nu \xi^\rho T_{\mu\rho} - \xi^\rho \partial_\rho T_{\mu\nu}. \end{aligned} \quad (8)$$

This leads to linear interactions with  $\pi$  of the form

$$\mathcal{L}_{\text{int}} = \alpha_1 \chi \dot{\pi} + \alpha_2 T_\mu^\mu \dot{\pi} + \alpha_3 T_{00} \dot{\pi} + \alpha_4 \left( M^2 T_{00} - 2\vec{T} \cdot \vec{\nabla} \pi \right), \quad (9)$$

where  $\vec{T} = T_{0i}$ . In the original ghost language, these couplings can be generated by writing down all Lorentz invariant couplings to  $\partial_\mu \phi$ , being careful to write down terms similar to equation (7). For more general tensor structures, it is far more efficient to work in the  $\phi$  language, and as shown in [1], the two languages give identical low energy Lagrangians. In general, for any Standard Model operator  $\mathcal{O}_{\mu\dots}$ , we expect to see a term  $M^2 \mathcal{O}_{0\dots}$  that explicitly breaks Lorentz- (and sometimes CPT-) invariance joined with a coupling between  $\nabla \pi$  and  $\mathcal{O}_{i\dots}$  that will lead to Lorentz-violating dynamics.

## 2.2 Effect of Gravitational Sources

In our analysis, we have assumed that we can always choose our coordinates such that the broken time-like diffeomorphism is in the coordinate time direction. Certainly at linearized level, the background  $\langle\phi\rangle = M^2 t$  is valid in any locally flat region, but the linearized approximation breaks down even around modest gravitational sources such as the earth. A more detailed analysis of the non-linearities will be carried out elsewhere [ref?], but we can quickly see why we expect non-linearities by the following argument.

A freely-falling observer will see the classical  $\phi$  field grow as  $M^2\tau$ , where  $\tau$  is the proper time in the observer's frame. If all observers began in the same inertial frame at zero velocity, then their worldlines would never cross and they would all agree on the value of  $\phi$  at any time slice. However, in the presence of a gravitational source, the worldlines of the observers would begin to cross, and except for the most symmetric situations, two crossed observers will have different values of their proper times, leading to caustics in the classical  $\phi$  field. The amount of time it takes these caustics to form is on the order of the gravitational infall time, which for the earth is around 20 minutes. These caustics are regions with very large  $\nabla\pi$ , and if the caustics are not smoothed out by non-linear effects, then when  $\nabla\pi \sim M^2$  the effective theory description breaks down because irrelevant operators dominate over relevant ones.

Even if the caustics are smoothed out, then from non-linear effects we have no reason to expect that  $\langle\phi\rangle = M^2 t$  in a cosmological rest frame is a good background for the  $\pi$  field in a local frame. In particular, we expect that the right background is  $\langle\phi\rangle = M^2 t + \epsilon(\vec{x})$ , where  $\epsilon(\vec{x})$  accounts for spacial inhomogeneities in the  $\phi$  field. However, it is easy to show that as long as the  $\phi$  background is smooth over some macroscopic length scale — such as the size of a laboratory or even possibly the size of a solar system — then the spacial inhomogeneities in  $\phi$  can be compensated by a local Galilean coordinate transformation, effectively redefining what is meant by the direction and magnitude of the ether wind. Therefore, in the remainder of the paper, when we talk about the velocity with respect to the ether rest frame, we are really referring to the local rest frame of  $\pi$  and not the cosmological rest frame of  $\pi$ . Of course, we also assume that we are far away from any possible caustics in order for the linear description to still hold.

## 2.3 Astrophysical Axion Constraints

The alert reader will notice that the second coupling in equation (2) looks a lot like the typical coupling of a pseudoscalar field. Weakly coupled pseudoscalar fields arise in models such as axions [ref?], and it is well known that there are considerable constraints on the size of these couplings coming from astrophysical bounds [ref?]. The mean free path of a weakly coupled particle is very long, so production of that particle can be the dominate mode of energy loss for an astrophysical object even if the rate of production is small, because energy can be lost from the entire volume of the object and not just from the surface. For example, if we naïvely translate the bound on axion couplings to electrons from studies of the energy loss of low-mass red-giants [ref?], we find that  $F > 10^9$  GeV.

However, we have to be careful about two things. First, the effective theory for  $\pi$  breaks down at an energy scale  $M$ , therefore we can only trust bounds coming from astrophysical objects whose typical temperature  $T$  is less than  $M$ . The bound quoted in [1] was  $M < 10$  MeV, but as we will emphasize in Section 2.4, we will consider much smaller  $M$  parameters. In any case, for  $M$  smaller than around 1 keV there are no relevant astrophysical bounds. Second, because the ghostone boson has a non-relativistic

dispersion relation, we need to understand the phase space of the  $\pi$  field in order to understand astrophysical cross sections. In general, cross sections are enhanced by a factor  $M/T$ , but there are some subtleties that will be explored elsewhere [ref?]. Until we have a better understanding of the phenomenologically viable range for  $M$  and of the cross sections for processes involving ghostone bosons, we will postpone the discussion of astrophysical constraints.

## 2.4 The $M$ Scale

In this paper, we will usually assume that  $M$  is between 1 eV and  $10^{-3}$  eV. Note that with such low  $M$  values, the IR modification of gravity due to mixing with the ghostone boson is heavily suppressed [1]. We have two different motivations for this  $M$  range. First, we might imagine that  $M$  is somehow a relevant cosmological scale. If  $M \sim 10^{-3}$  eV, then ghost condensation could explain the observed acceleration of the universe even if the cosmological constant were zero. Alternatively,  $M \sim 1$  eV is around the temperature of matter domination in our universe, perhaps indicating that the ghost condensate is a dark matter candidate.

Second, small values of  $M$  will lead to big effects when the ghostone boson is coupled directly to Standard Model fermions. If we are moving with a velocity  $v$  relative to the ether rest frame, then we will see that  $1/Mv$  sets the scale for Lorentz-violating dynamics. If the ether rest frame is the same as the rest frame of the cosmic microwave background then  $v \sim 10^{-3}$ , setting a *macroscopic* length scale somewhere between a tenth of a millimeter and tens of centimeters! Of course, there is no reason why  $M$  could not be much larger than these scales, but in the spirit of unabashed optimism, we will assume that the scale  $M$  is both cosmologically relevant and well-suited to experiments.

## 2.5 Couplings to the Standard Model

Even if the ghostone boson does not coupling to the Standard Model at tree level, we are guaranteed that couplings will be generated through graviton loops. In particular, if  $\mathcal{O}^{\mu\nu}$  is a symmetric dimension four Standard Model operator, then there is no symmetry forbidding the coupling

$$\mathcal{L}_{\text{int}} \sim \frac{1}{M_{\text{Pl}}^4} \mathcal{O}^{\mu\nu} \partial_\mu \phi \partial_\nu \phi \rightarrow \frac{M^4}{M_{\text{Pl}}^4} \mathcal{O}_{00} - 2 \frac{M^2}{M_{\text{Pl}}^4} \mathcal{O}_{0i} \nabla_i \pi + \dots \quad (10)$$

One interesting candidate for  $\mathcal{O}^{\mu\nu}$  is the stress-energy tensor  $T^{\mu\nu}$ . This generates a coupling between matter and the ghostone boson beyond the minimal gravitational coupling. Indeed we recognize  $T^{0i}$  as the momentum density, so in addition to the velocity-dependent modification to Newton's law due to mixing between gravity and the ghostone boson, there is apparently a secondary (and *very* small) momentum-dependent modification.

The companion term  $(M/M_{\text{Pl}})^4 T_{00}$  is also quite interesting. For a Dirac fermion (assuming gauge couplings are set to zero), the symmetric stress-energy tensor is

$$T^{\mu\nu} = \frac{i}{2} \bar{\Psi} (\gamma^\mu \partial^\nu + \gamma^\nu \partial^\mu) \Psi - \eta^{\mu\nu} \bar{\Psi} (i \gamma^\rho \partial_\rho - m) \Psi \quad (11)$$

The effect of adding the operator  $(M/M_{\text{Pl}})^4 T_{00}$  to the Lagrangian is to modify the dispersion relation for the fermion to

$$\omega^2 = \left(1 - c \frac{M^4}{M_{\text{Pl}}^4}\right) (k^2 + m^2), \quad (12)$$

where  $c$  is an order one coefficient (possibly negative). This has the effect of changing the maximum attainable velocity for the fermion, and the known bound from the absence of vacuum Cherenkov radiation for protons [ref?] is

$$\frac{M^4}{M_{\text{Pl}}^4} < 10^{-23}. \quad (13)$$

This places a trivial bound  $M < 10^{13}$  GeV.

Clearly, any Lorentz- or CPT-violations mediated to the Standard Model by graviton loops will be very small, so it is worth considering the effect of direct couplings to the ghostone boson. These couplings were considered in [1], but we will review them here as well. In the non-relativistic limit, couplings to scalar operators are not interesting because they involve the time derivative of  $\pi$ , which is assumed to be much smaller than  $\nabla\pi$ . The leading coupling to the Standard Model comes from any dimension three vector operator  $J^\mu$ :

$$\mathcal{L}_{\text{int}} = \frac{1}{F} J^\mu \partial_\mu \phi \rightarrow \frac{1}{F} (M^2 J_0 + J^\mu \partial_\mu \pi). \quad (14)$$

(For simplicity, we are ignoring the lesson of Section 2.1 and assuming that  $F = F'$ . In the non-relativistic limit, this will not make any difference.) Note that this coupling could be forbidden by a  $\phi \rightarrow -\phi$  symmetry. In the Goldstone boson language, this is equivalent to imposing time reversal invariance in addition to  $SO(3)$  invariance. Still, this is the leading coupling that could mediate Lorentz- and CPT-violations to the Standard Model, and we really have no *a priori* reason for excluding it.

If we do break time reversal invariance, however, then the kinetic terms for  $\pi$  from equation (1) are slightly modified. In this paper, we will ignore this modification because it does not change the fact that the on-shell condition for the ghostone still implies that  $\omega \sim k^2$ , so at least at a qualitative level, the Lorentz-violating dynamics will be unchanged.

The most general vector operator we can create from Standard Model fermions is

$$J^\mu = \sum_{\psi} c_{\psi} \bar{\psi} \vec{\sigma}^{\mu} \psi, \quad (15)$$

where we have assumed that fermions with the same quantum numbers have been diagonalized to the “ghostone boson interaction” basis. The couplings in equation (14) can actually be removed via a field redefinition

$$\psi \rightarrow e^{i c_{\psi} \phi / F} \psi, \quad (16)$$

but if there are Dirac mass terms or other interactions in the action that break this  $U(1)$  symmetry, then some part of the interaction will remain. For concreteness, consider two fermion fields  $\psi$  and  $\psi^c$  that are joined by a Dirac mass term  $m_D \psi \psi^c$ . This mass term preserves the vector  $U(1)$  symmetry but breaks the axial  $U(1)$  symmetry, therefore the coupling to the fermion vector current can be removed but the coupling to the fermion axial current remain.

In particular, we are left with (in Dirac notation)

$$\mathcal{L}_{\text{int}} \sim \frac{1}{F} \bar{\Psi} \gamma^{\mu} \gamma^5 \Psi \partial_{\mu} \phi \rightarrow \mu \bar{\Psi} \gamma^0 \gamma^5 \Psi + \frac{1}{F} \bar{\Psi} \gamma^{\mu} \gamma^5 \Psi \partial_{\mu} \pi, \quad \mu = \frac{M^2}{F}. \quad (17)$$



The first term violates Lorentz- and CPT-invariance and gives rise to different dispersion relations for left- and right-helicity particles and antiparticles [ref?],

$$\omega^2 = (|k| \pm \mu)^2 + m_D^2, \quad (18)$$

where the plus sign is for left-helicity particles and antiparticles, and the minus sign is for right-helicity particles and antiparticles. Also, if the earth is moving with respect to the ether rest frame, then after a Lorentz boost, the first term looks like the interaction

$$\mu \bar{\Psi} \vec{\gamma} \gamma^5 \Psi \cdot \vec{v}_{\text{earth}}. \quad (19)$$

In the non-relativistic limit, the current  $\bar{\Psi} \vec{\gamma} \gamma^5 \Psi$  is identified with the spin density  $\vec{s}$ , giving us a direct coupling between the velocity of the earth and fermion spin

$$\mu \vec{s} \cdot \vec{v}_{\text{earth}}. \quad (20)$$

Experimental limits on such couplings have placed considerable bounds on  $\mu$ . If we assume that the rest frame of the ghostone is the same as the rest frame of the cosmic microwave background, then  $|\vec{v}_{\text{earth}}| \sim 10^{-3}$ . The bound on couplings to electrons is  $\mu < 10^{-25}$  GeV [ref?] and to nucleons  $\mu < 10^{-24}$  GeV [ref?]. Because  $\mu = M^2/F$ , we can use these bounds to place limits on the parameters of our theory. For example, if we thought that the coupling between the ghostone and the electron were set at the Planck scale, then naturalness suggests  $F \sim 10^{19}$  GeV giving the bound  $M < 1$  MeV. Note that  $F$  could be much higher than the Planck scale if the coupling to the ghostone came from integrating out many particles above the scale  $M$ .

The second interaction in equation (17) leads to the interesting Lorentz-violating dynamics and will be the focus of the remainder of the paper. In the non-relativistic limit

$$\mathcal{L}_{\text{int}} = \frac{1}{F} \vec{s} \cdot \vec{\nabla} \pi. \quad (21)$$

This coupling is familiar from axions, because it is a generic coupling between fermions and Goldstone bosons. What makes this different from the standard story for Goldstone bosons is that the ghostone has a Lorentz-violating  $\omega \sim k^2/M$  dispersion relation. The exchange of a normal Goldstone boson between spin sources leads to a  $1/r^3$  spin-dependent potential, but as we will see in Section 4, the exchange of a ghostone boson leads to a  $1/r$  potential! Even more amazing, there is a new dynamical process that is usually absent in the context of Goldstone bosons but is familiar from electromagnetism. This process is ether Cherenkov radiation.

### 3 Ether Cherenkov Radiation

In classical electrodynamics, Cherenkov radiation occurs when a charged particle moves through a medium at velocities higher than the speed of light in that medium. It can be thought of as the optical analog of a sonic boom. By energy conservation, the charged particle must lose energy in order to generate the photonic shockwave, and once the particle's velocity is less than the medium's light speed, the Cherenkov radiation ceases.

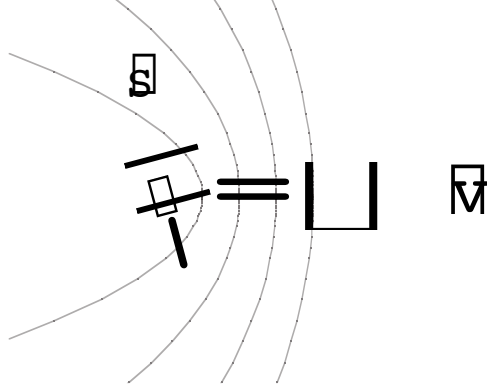


Figure 1: A cartoon of ether Cherenkov radiation. The spin  $\vec{S}$  is traveling at velocity  $\vec{v}$  relative to the ether rest frame. Gray lines are meant to be suggestive of ghostone shockwaves.

In the case of the ghostone boson, its dispersion relation is  $\omega \sim k^2/M$ , so the velocity for ghostone boson excitations is

$$v \sim \frac{\omega}{k} = \frac{k}{M}. \quad (22)$$

For a particle traveling at some fixed velocity, there is always a  $k$  such that the speed of the ghostone is less than the speed of the particle. As shown in Figure 1, we expect that a particle in motion relative to the ether rest frame — and which couples to the ghostone boson — will radiate away energy until it is at rest with respect to the ether wind.

With usual Cherenkov radiation, we can use photon detectors to study the photonic shockwave and use that information to understand the motion of the charged particles. Unfortunately, we do not (yet) have ghostone boson detectors, so the most likely experimental signature of ether Cherenkov radiation would be slight, unexplained kinetic energy loss for particles with spin. More precisely, depending on the velocity of the observed particle and the velocity of the laboratory frame with respect to the ether rest frame, we would see kinetic energy losses or gains.

We can use a trick to calculate  $dE/dt$  for the particle in motion, namely the amount of power needed to maintain the particle's kinetic energy despite the ether drag. The equation of motion for the ghostone boson in the presence of a spin source is

$$\ddot{\pi} + \frac{1}{M^2} \nabla^4 \pi = -\frac{1}{F} \vec{\nabla} \cdot \vec{s}. \quad (23)$$

Multiplying both sides by  $\dot{\pi}$ , integrating over all space, and rewriting:

$$\frac{d}{dt} \left( \int d^3r \frac{1}{2} \dot{\pi}^2 + \frac{1}{2M^2} (\nabla^2 \pi)^2 \right) = \frac{1}{F} \int d^3r \vec{s} \cdot \vec{\nabla} \dot{\pi}. \quad (24)$$

We recognize the term in parenthesis as the “particle physics” energy of the ghostone boson field. Any energy that goes into the  $\pi$  field is energy that we would need to pump into the moving spin to maintain its velocity relative to the ether. Therefore, the rate of energy loss by the moving spin due to ether Cherenkov radiation is

$$\frac{dE_{\text{spin}}}{dt} = -\frac{1}{F} \int d^3r \vec{s} \cdot \vec{\nabla} \dot{\pi}. \quad (25)$$

We will first calculate this energy dissipation for a spin-density corresponding to a point-like spin moving with velocity  $\vec{v}$  relative to the ether:

$$\vec{s} = \vec{S} \delta^{(3)}(\vec{r} - \vec{v}t), \quad \vec{s} = (2\pi)\vec{S} \delta(w - \vec{k} \cdot \vec{v}). \quad (26)$$

Using Greens functions, the classical solution to equation (23) in momentum space is

$$\tilde{\pi}(\omega, \vec{k}) = \frac{1}{F} \frac{-i\vec{k} \cdot \vec{s}}{(\omega + i\epsilon)^2 - k^4/M^2}, \quad (27)$$

where the  $i\epsilon$  insures that we are using the retarded Greens function. Plugging this into the energy dissipation formula in equation (25),

$$\frac{dE_{\text{spin}}}{dt} = \frac{iM^2}{F^2} \int \frac{k^2 dk d\Omega_k}{(2\pi)^3} \frac{k^3}{k^2} \frac{(\vec{S} \cdot \hat{k})^2 (\hat{k} \cdot \vec{v})}{(M\hat{k} \cdot \vec{v} + i\epsilon/k)^2 - k^2}. \quad (28)$$

At first, it looks like this expression might be zero because it is odd in  $k$ , but notice there are poles at  $k = \pm M\hat{k} \cdot \vec{v} + i\epsilon$ . (We choose our integration ranges such that  $\hat{k} \cdot \vec{v}$  is always positive.) In fact, we see exactly what the poles mean; when the velocity of the source is such that the ghostone boson can “go on-shell” then there is Cherenkov radiation, and this is the always the case for a non-zero  $v$ . Our pole prescription guarantees that the moving particle is radiating  $\pi$  energy away to infinity as opposed to receiving  $\pi$  radiation from infinity.

$$\frac{dE_{\text{spin}}}{dt} = -\frac{M^4}{F^2} \frac{|v|}{96\pi} \left( |S|^2 |v|^2 + 3(\vec{S} \cdot \vec{v})^2 \right). \quad (29)$$

We see that the rate of energy loss is roughly proportional to  $v^3$  and depends on the orientation of the spin with respect to the ether wind. We can use this result to estimate the expected kinetic energy loss for the most abundant spin point source: an electron. Note that we already have a bound on  $M^2/F$  of  $10^{-25}$  GeV and the spin of an electron is  $1/2$ , so if we assume that  $|v| \sim 10^{-3}$ ,

$$\frac{dE_{\text{electron}}}{dt} < 10^{-37} \text{ GeV s}^{-1}. \quad (30)$$

This is an incredibly small energy change over a very long period of time, so it is unlikely that we will ever have the experimental precision to track the energy loss of a single electron.

In order to see a measurable effect from ether Cherenkov radiation, we need to have a large value of  $S$ . However, it is not enough to simply have a source with a large magnetic moment, as orbital angular momentum generically couples more weakly to  $\pi$  than spin. In particular, the magnetic moment of the earth is not due to spin alignment, so it is not an effective  $\pi$  radiator. Neutron stars are large astrophysical spin sources; a neutron star with the same mass as the sun has a net spin  $S \sim 10^{56}$  inside a radius  $R \sim 1$  km. Closer to home, a 1 ton Alnico magnet has a net spin  $S \sim 10^{28}$  inside a radius  $R \sim .5$  m. Because the spin of these types of objects is spread out over a finite region, we expect the ether drag to be suppressed by some factor of the radius of the source.

For simplicity, consider a rectangle function source:

$$\vec{s} = \frac{\vec{S}}{\frac{4}{3}\pi R^3} \begin{cases} 1 & |\vec{r} - \vec{v}t| < R \\ 0 & |\vec{r} - \vec{v}t| > R \end{cases}. \quad (31)$$

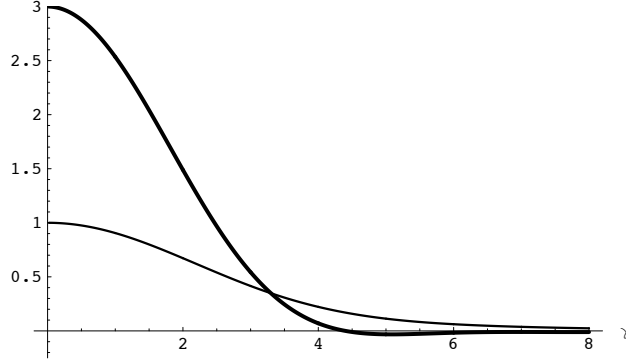


Figure 2: The suppression of ether Cherenkov radiation due to finite sources from equation (32),  $\gamma = MRv$ . The light curve is  $C(\gamma)$  and the bold curve is  $D(\gamma)$ . Note that they reproduce the result from equation (29) when  $\gamma \rightarrow 0$ .

(We have also considered a Gaussian distribution and the results are nearly identical up to logarithmic factors.) Following the exact same logic as above:

$$\frac{dE_{\text{rectangle spin}}}{dt} = -\frac{M^4 |v|}{F^2 96\pi} \left( C(\gamma) |S|^2 |v|^2 + D(\gamma) (\vec{S} \cdot \vec{v})^2 \right). \quad (32)$$

where  $\gamma = MRv$ . Plots of  $C(\gamma)$  and  $D(\gamma)$  for small  $\gamma$  appear in Figure 2. For large  $\gamma$ , the functions behave as

$$C(\gamma) \sim \frac{54 \log \gamma}{\gamma^4}, \quad D(\gamma) \sim -\frac{54 \log \gamma}{\gamma^4}. \quad (33)$$

If we assume that  $M \sim 10^{-3}$  eV, then the neutron star has  $\gamma \sim 5000$  and the 1 ton Alnico magnet has  $\gamma \sim 5$ . Using the bound  $M^2/F \sim 10^{-25}$  GeV, we see that the neutron star would lose all of its kinetic energy relative to the ether rest frame ( $E = \frac{1}{2}mv^2$ ) in just  $10^{-10}$  seconds, and the Alnico magnet would lose all of its kinetic energy in about a week.

This means that for this value of  $M$ ,  $M^2/F$  cannot saturate the experimental bound. As we will see in Section 5, the effective theory breaks down around large sources unless  $F$  is small enough. If we keep  $M$  fixed, then for the neutron star  $M^2/F$  cannot exceed  $10^{-59}$  GeV, and for the Alnico magnet  $M^2/F$  cannot exceed  $10^{-38}$  GeV. In both cases, the time to see any measurable decrease in kinetic energy is longer than the age of the universe. As we will see, by increasing  $M$  it is possible to have much higher values of  $M^2/F$ , but at the cost of increasing the  $\gamma$  suppression factors. At the end of the day, it seems highly unlikely that we could observe the effects of ether Cherenkov radiation.

## 4 Long-Range Spin-Dependent Potential

The most well known long-range spin-dependent potential is the  $1/r^3$  potential transmitted by magnetic fields. As shown in [5], there is also a  $1/r^3$  potential coming from pseudoscalar bosons such as axions. Consider a massless spin-0 field  $\varphi$  that has a normal  $\omega \sim k$  dispersion relation and a coupling to the fermion

axial current,  $\vec{s} \cdot \vec{\nabla} \varphi / F$ . In the Born approximation, the potential between two point spins is the Fourier transform of the propagator times the couplings with  $\omega \rightarrow 0$ .

$$V_\varphi(r) = \frac{1}{F^2} \int \frac{d^3k}{(2\pi)^3} \frac{(-i\vec{k} \cdot \vec{S}_1)(-i\vec{k} \cdot \vec{S}_2)}{k^2} e^{i\vec{k} \cdot \vec{r}} = \frac{-1}{F^2} (\vec{S}_1 \cdot \vec{\nabla})(\vec{S}_2 \cdot \vec{\nabla}) \int \frac{d^3k}{(2\pi)^3} \frac{1}{k^2} e^{i\vec{k} \cdot \vec{r}} \quad (34)$$

The Fourier transform of  $1/k^2$  is well-known.

$$V_\varphi(r) = \frac{-1}{F^2} (\vec{S}_1 \cdot \vec{\nabla})(\vec{S}_2 \cdot \vec{\nabla}) \frac{1}{4\pi r} = \frac{1}{4\pi F^2} \frac{(\vec{S}_1 \cdot \vec{S}_2) - 3(\vec{S}_1 \cdot \hat{r})(\vec{S}_2 \cdot \hat{r})}{r^3} \quad (35)$$

The form of this potential is identical to the potential between magnetic dipoles in electromagnetism, so it would be very difficult to resolve the pseudoscalar effect from the magnetic effect.

In the case of the ghostone boson, we have an  $\omega \sim k^2/M$  dispersion relation, so if our sources are in the ether rest frame, the spin-spin potential goes as

$$V_\pi(r) = \frac{-1}{F^2} (\vec{S}_1 \cdot \vec{\nabla})(\vec{S}_2 \cdot \vec{\nabla}) \int \frac{d^3k}{(2\pi)^3} \frac{M^2}{k^4} e^{i\vec{k} \cdot \vec{r}} = \frac{M^2}{F^2} (\vec{S}_1 \cdot \vec{\nabla})(\vec{S}_2 \cdot \vec{\nabla}) \frac{r}{8\pi}. \quad (36)$$

Expanding the derivatives:

$$V_\pi(r) = \frac{M^2}{8\pi F^2} \frac{(\vec{S}_1 \cdot \vec{S}_2) - (\vec{S}_1 \cdot \hat{r})(\vec{S}_2 \cdot \hat{r})}{r}. \quad (37)$$

The novel dispersion relation for the ghostone has produced a long-range  $1/r$  potential between spins! Assuming that  $M/F$  is not too small, we should be able to design experiments to measure this force.

Before we get too excited, there are a few things we need to check. In any real experiment we will be dealing with finite sources traveling with some velocity with respect to ether wind, and just like the example of Cherenkov radiation, we expect to see some  $\gamma = MRv$  suppression factors. But even putting that aside, we need to understand what the Born approximation really means in this context. By taking  $\omega \rightarrow 0$ , we are assuming that  $\omega \ll k^2/M$ . In position space, this means that our approximation is only valid on time scales

$$t \gg Mr^2. \quad (38)$$

For a normal  $\omega \sim k$  dispersion relation, we have to only wait a time  $t = r$  for our system to behave “non-relativistically”. For the ghostone mediated forces, however, the time to reach steady state is increased by a factor of  $Mr$ . For an  $M$  of 1 eV, this factor is  $r/(10^{-5} \text{ cm})$  which, given the speed of light, is negligible for any reasonably sized experiment. However, because we also want to understand ghostone dynamics for much larger values of  $M$ , we want to study how the spin-spin force evolves over time.

Consider a spin source at the origin that turns on at  $t = 0$ :

$$\vec{s} = \vec{S}_1 \delta^{(3)}(\vec{r}) \theta(t). \quad (39)$$

(We have also looked at a spin source that smoothly turns on, and the following results are robust against possible transient effects.) Assuming a test spin  $\vec{S}_2$  sitting at  $\vec{r}$ , the expression for  $V_\pi(r, t)$  is

$$\begin{aligned} V_\pi(r, t) &= \frac{-1}{F^2} (\vec{S}_1 \cdot \vec{\nabla})(\vec{S}_2 \cdot \vec{\nabla}) \int d^3r_0 dt_0 \delta^{(3)}(\vec{r}_0) \theta(t_0) \int \frac{d^3k dw}{(2\pi)^4} \frac{1}{(w + i\epsilon)^2 - k^4/M^2} e^{i\vec{k} \cdot (\vec{r} - \vec{r}_0)} e^{-iw(t - t_0)} \\ &= \frac{-1}{F^2} (\vec{S}_1 \cdot \vec{\nabla})(\vec{S}_2 \cdot \vec{\nabla}) \int \frac{d^3k}{(2\pi)^3} \frac{M^2}{k^4} (1 - \cos(tk^2/M)) e^{i\vec{k} \cdot \vec{r}}, \end{aligned} \quad (40)$$

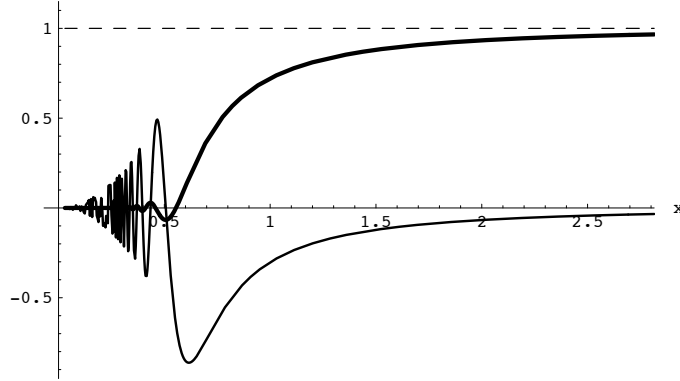


Figure 3: The time evolution of the long-range spin-dependent potential from equation (41),  $x = t/Mr^2$ . The bold curve is  $K(x)$  and the light curve is  $L(x)$ . Note that these functions reproduce the result from equation (37) in the large  $x$  limit.

where again we have used a pole prescription corresponding to the retarded potential. For large  $t$ , the oscillatory part of the integral vanishes, and we recover the result from equation (36). When  $t = 0$ , the potential is zero, as we would expect because information about  $\vec{S}_1$  has not yet reached  $\vec{S}_2$ . If we had a normal  $\omega \sim k$  dispersion relation, then the potential would turn on suddenly when  $t = r$ . Here, however, there is no Lorentz invariance, so we have no reason to expect a vanishing potential outside the light-cone. More precisely, the effective theory breaks down for  $k > M$ , and because we are not imposing a momentum cutoff, we are inadvertently propagating modes that travel faster than light.

The time-dependent potential is

$$V_\pi(r, t) = \frac{M^2}{8\pi F^2} \left( K(x) \frac{\vec{S}_1 \cdot \vec{S}_2 - (\vec{S}_1 \cdot \hat{r})(\vec{S}_2 \cdot \hat{r})}{r} + L(x) \frac{(\vec{S}_1 \cdot \hat{r})(\vec{S}_2 \cdot \hat{r})}{r} \right), \quad (41)$$

where  $x = t/Mr^2$ . Plots of  $K(x)$  and  $L(x)$  functions appear in Figure 3. We see that the potential does not come to its full value until  $t \sim Mr^2$ . For  $t$  small compared to  $Mr^2$ , the potential oscillates between being attractive and repulsive. The envelope for the oscillations are

$$|K(x)| \sim 2.3x^2, \quad |L(x)| \sim 4.5x^6. \quad (42)$$

Because the potential behaves so erratically for small  $x$  values, a realistic experiment will probably have to wait until  $x \gg 1$  to see a coherent effect. In the long time limit

$$K(x) \sim 1 - \frac{.27}{x^2}, \quad L(x) \sim -\frac{.27}{x^2}. \quad (43)$$

Now we consider the effect of finite sources moving with some velocity with respect to the ether rest frame. In particular, experiments on the earth with magnets fixed to the surface of the earth would be described by sources moving together with a slowly varying velocity  $v$ . We might expect that if the source and test spin are traveling fast with respect to the ether, then the  $\pi$  waves would not be able to “keep up”, and the spin-spin potential would be suppressed. What we will actually find is far more interesting.

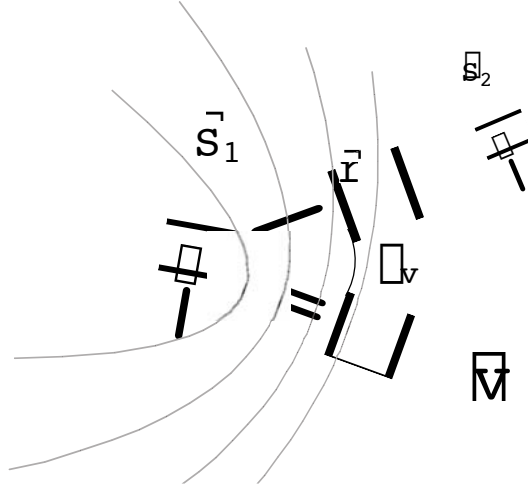


Figure 4: A cartoon of the vectors involved in the long-range spin-dependent potential. Gray lines are meant to be suggestive of peaks and troughs in the potential.  $\vec{S}_1$  is the source spin moving with velocity  $\vec{v}$ .  $\vec{S}_2$  is a co-moving test spin a distance  $r$  away.

The finite source is

$$\vec{s} = \frac{\vec{S}_1}{\frac{4}{3}\pi R^3} \begin{cases} 1 & |\vec{r} - \vec{v}t| < R \\ 0 & |\vec{r} - \vec{v}t| > R \end{cases} . \quad (44)$$

Following Figure 4, we want to look at the co-moving potential, namely the potential between  $\vec{S}_1$  and some test spin  $\vec{S}_2$  that is moving at the same velocity as  $\vec{S}_1$ . The potential at a co-moving distance  $r$  is

$$V(r) = \frac{M^2}{F^2} (\vec{S}_1 \cdot \vec{\nabla})(\vec{S}_2 \cdot \vec{\nabla}) \int \frac{d^3k}{(2\pi)^3} \frac{e^{i\vec{k}\cdot\vec{r}}}{(M\vec{k} \cdot \vec{v} + i\epsilon)^2 - k^4} \frac{3(\sin kR - kR \cos kR)}{(kR)^3} \quad (45)$$

As expected, when  $v = 0$  and  $R = 0$ , we recover the zero-velocity result from equation (36). Evaluating derivatives:

$$V(r) = \frac{M^2}{8\pi F^2} \left( A(\alpha, \gamma, \theta_v) \frac{\vec{S}_1 \cdot \vec{S}_2 - (\vec{S}_1 \cdot \hat{r})(\vec{S}_2 \cdot \hat{r})}{r} + B(\alpha, \gamma, \theta_v) \frac{(\vec{S}_1 \cdot \hat{r})(\vec{S}_2 \cdot \hat{r})}{r} \right), \quad (46)$$

where  $\alpha = Mrv$ ,  $\gamma = MRv$ , and  $\cos \theta_v = \hat{r} \cdot \hat{v}$ . The actual functional forms of  $A$  and  $B$  are not particularly enlightening, so we will evaluate them in certain limits to get an idea of their behavior.

We will start with the case  $\theta_v = 0$ . When  $\gamma = 0$ , there is a nice analytic form for  $A$  and  $B$ .

$$A(\alpha, 0, 0) = \begin{cases} 2 \sin \alpha / \alpha & \alpha > 0 \\ 0 & \alpha < 0 \end{cases}, \quad B(\alpha, 0, 0) = \begin{cases} 2(\cos \alpha - \sin \alpha / \alpha) & \alpha > 0 \\ 0 & \alpha < 0 \end{cases}. \quad (47)$$

We see that at finite velocity the potential oscillates between being attractive and repulsive as  $r$  varies! Note that there is a potential only *in front* of the spin source. While this is a bit counter-intuitive — naïvely, we might expect a spin source to leave a potential in its wake — the result is consistent because the source is traveling at subluminal velocities whereas the potential is generated by  $\pi$  waves that can propagate as fast as the speed of light. Still, it is a bit bizarre that potential is identically zero behind the

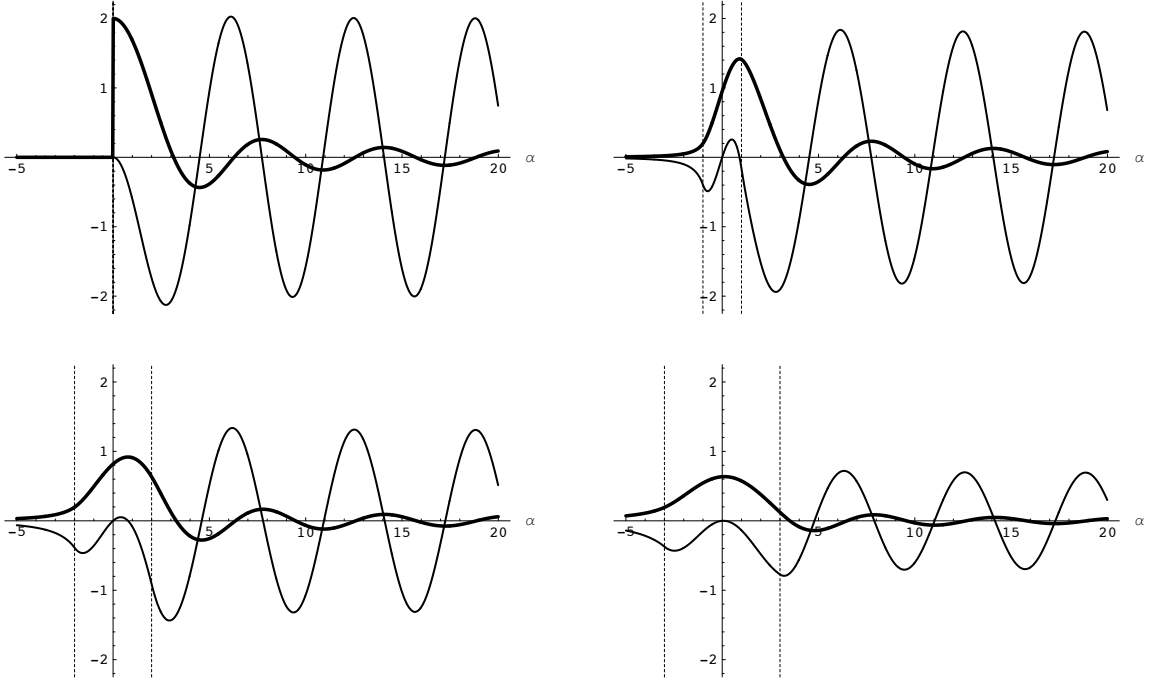


Figure 5: The effect of finite sources on the long-range spin-dependent potential from equation (46),  $\alpha = Mrv$  and  $\gamma = MRv$ . The bold curves are  $A(\alpha, \gamma, \theta_v = 0)$  and the light curves are  $B(\alpha, \gamma, \theta_v = 0)$  for  $\gamma = 0, 1, 2,$  and  $3$ . Dashed lines indicate the size of the source.

source, but this result is softened when we introduce finite sized sources. Also, note that the component of the potential that survives at zero velocity (the  $A$  piece) damps out for large  $\alpha$  whereas the component of the potential that is absent at zero velocity (the  $B$  piece) has an oscillatory amplitude that does not vanish for large  $\alpha$ . The factor of two in equation (47) tells us that the zero velocity potential ( $\alpha \rightarrow 0$ ) is recovered by taking the average of the potential at negative  $\alpha$  and positive  $\alpha$ .

In Figure 5 we see the effect of introducing finite sources, namely to “average” over the oscillations in equation (47). For sufficiently small  $\gamma$ , the shape of the potential is not significantly modified but the amplitude is somewhat suppressed. If we consider  $M \sim 10^{-3}$  eV, then  $1/Mv$  is on the order of tens of centimeters, and we can certainly imagine constructing a spin source such that  $\gamma$  is  $\mathcal{O}(1)$ . For large  $\gamma$ , the potential is generically suppressed by  $1/\gamma^2$ , though for  $\alpha$  negative and near  $\gamma$ , the suppression is only by  $1/\gamma^{3/2}$ . In general, it is difficult to make hard predications at large  $\gamma$  because the shape of the potential is sensitively dependent on the spin distribution in the finite source.

If we assume that  $\gamma = 0$ , then the most spectacular prediction of ghostone mediated spin potentials is the angular dependence. In Figure 6, we see the value of the  $A$  and  $B$  components of the potential as a function of  $\alpha$  and  $\theta_v$ . In a realistic situation, both the  $A$  and  $B$  components would vanish for sufficiently large  $\alpha$  because as we saw in Figure 3, it takes a time  $t \sim Mr^2$  for the potential to reach steady state. Presumably, by mapping out the potential for various orientations of the spins it would be possible to determine the direction of the ether wind and the value of  $Mv$ .



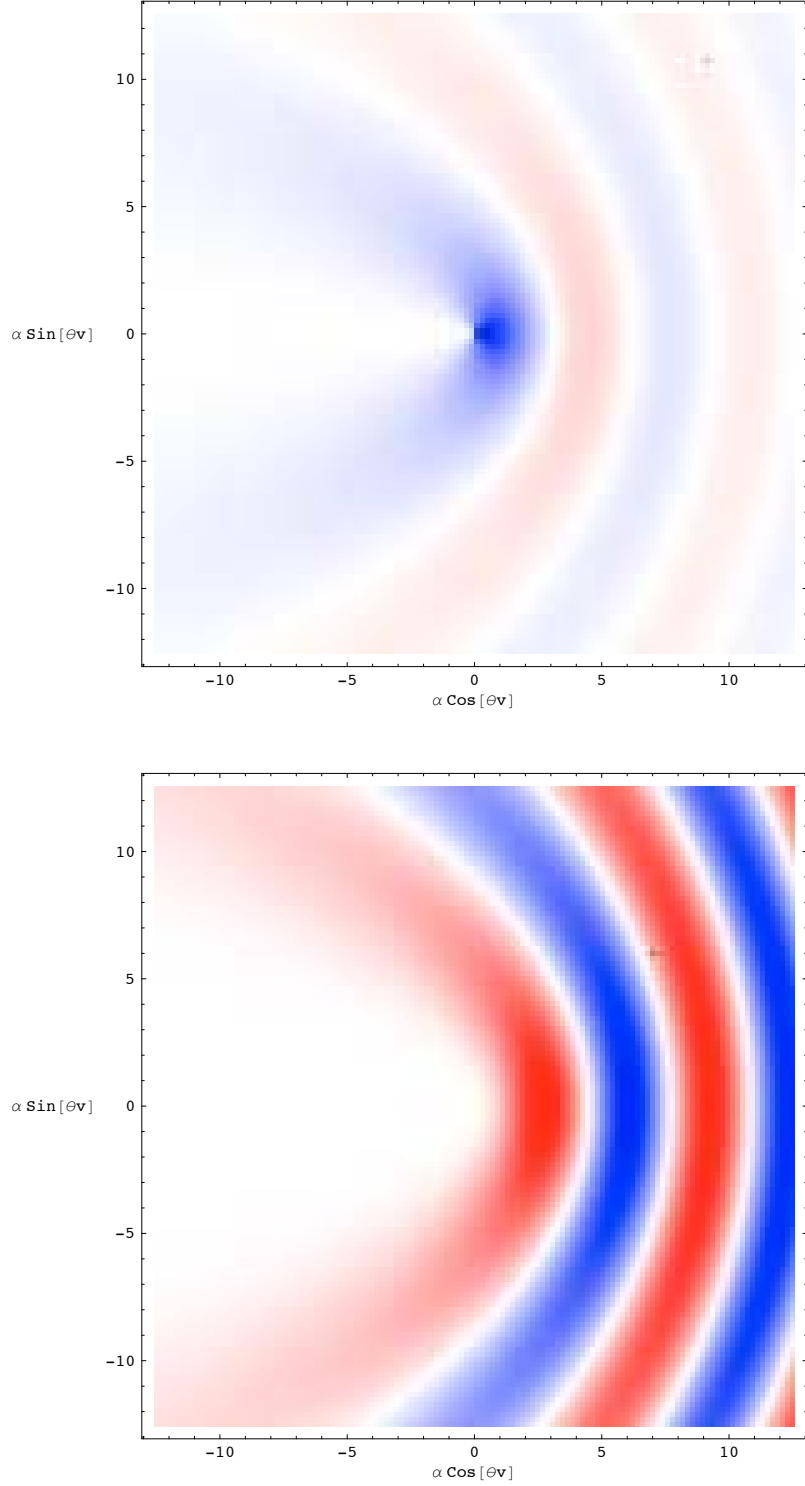


Figure 6: The angular dependence of the long-range spin dependent potential from equation (46),  $\alpha = Mrv$  and  $\cos \theta_v = \hat{r} \cdot \hat{v}$ . The top function is  $A(\alpha, \gamma = 0, \theta_v)$  and the bottom function is  $B(\alpha, \gamma = 0, \theta_v)$ . Blue indicates positive potential, red indicates negative potential, and white indicates zero potential. The parabolic shape of the potential peaks and troughs are a direct consequence of the  $\omega \sim k^2/M$  dispersion relation for the ghostone boson. It is also intuitively obvious that the “ether wind” is blowing to the left.

Unlike ether Cherenkov radiation where the only experimental signal was slight kinetic energy variation, we can see the ghostone boson in the case of the long-range spin-dependent potential by mapping out the potential as a function of  $\theta_v$ . Even if our spin source and test spin were fixed to the surface of the earth, the value of  $\theta_v$  would still vary over the course of a day! As we will see in Section 5, the magnitude of the spin-dependent potential is generically much weaker than gravity, but because the angular dependence is so different from gravity or even magnetism, it should be possible to extract the ghostone boson component of any  $1/r$  potential, because as is evident from Figure 6, the ghostone boson potential defines a preferred axis in space.

## 5 Limits on the Effective Theory

As a final check that our analysis makes sense, we need to verify that adding large sources does not push the ghostone boson out of the range of validity for the effective theory. In particular, when

$$\nabla\pi \sim M^2, \quad (48)$$

then our theory loses predictability because irrelevant operators make large, unknown contributions to the action. This is not the only concern, however. Even if the theory has predictability, large sources might push us out of the linear regime. The least irrelevant interaction for the ghostone boson in the static limit ( $\dot{\pi} = 0$ ) is  $(\nabla\pi)^4/M^4$ , and if this term is larger than the source term  $\vec{s} \cdot \vec{\nabla}\pi/F$ , then self-interactions dominate over sources. In particular,  $|\vec{s}| \sim S/R^3$  so non-linear effects become important when

$$\frac{(\nabla\pi)^3}{M^4} \sim \frac{S}{FR^3}. \quad (49)$$

In this case, while the effective theory may still be well-behaved, our linearized analysis is no longer valid because we have ignored non-linear terms in the equation of motion for the ghostone boson.

We can easily calculate the maximum magnitude of  $\nabla\pi$  for the source in equation (44). Note that  $\nabla\pi$  in a comoving frame is the same as  $\nabla\pi$  is the ether rest frame, because in the non-relativistic limit the two frames are connected by a Galilean transformation which does not affect spacial derivatives. For large finite sources, the maximum value of  $\nabla\pi$  happens to occur directly behind the spin source:

$$|\nabla\pi| \sim \frac{SM^2}{FR} \frac{1}{\gamma^{3/2}}, \quad (50)$$

where again  $\gamma = MRv$  and  $R$  is the radius of the source. If  $\gamma \sim \mathcal{O}(1)$ , then we can just drop the  $\gamma$  suppression factor. The bounds on the size of the source are

$$S_{\text{no predictability}} \sim FR\gamma^{3/2}, \quad S_{\text{non-linear}} \sim \frac{F}{M}\gamma^{9/4}. \quad (51)$$

Note that just because there may exist a spin source that violates these bounds, it does not mean that we can use this information to place constraints on  $M$  and  $F$ . In our entire analysis, we are assuming that full diffeomorphism invariance is restored in the UV, so the irrelevant interactions of the ghostone boson must somehow encode the fact that Lorentz symmetry is actually a good symmetry of the complete theory.

Therefore, though we cannot trust the theory of ghostone bosons around large sources, the fact that large sources exist does not mean that the ghostone description is not valid around smaller sources.

We are now ready to see the phenomenologically viable and experimentally testable regions of our parameter space. The strength of the long-range spin-dependent potential goes as  $(M/F)^2$ , so it is convenient to place bounds in terms of  $M/F$  and  $M$ . In order to realize the spectacular predictions from Figure 6, we want a source for which  $\gamma$  is  $\mathcal{O}(1)$ . In other words we want to choose  $R \sim 1/Mv$ . If we take an Alnico magnet as the canonical spin source, then

$$S \sim R^3 \left( \frac{10^{23} \text{ spins}}{\text{cm}^3} \right) \sim \left( \frac{10^{-6} \text{ GeV}}{Mv} \right)^3. \quad (52)$$

Note that as  $Mv$  increases, the total spin must decrease in order for  $\gamma$  to remain  $\mathcal{O}(1)$ . Plugging this into equation (51) assuming  $v \sim 10^{-3}$ , we find the following constraints on  $M/F$  and  $M$ .

$$\frac{M}{F} < \left( \frac{M}{10^{-4} \text{ GeV}} \right)^3 \quad (\text{to be predictive}), \quad \frac{M}{F} < \left( \frac{M}{10^{-3} \text{ GeV}} \right)^3 \quad (\text{to be linear}). \quad (53)$$

Combining this information with the experimental bound  $M^2/F \sim 10^{-25} \text{ GeV}$ , Figure 7 shows the experimental testable region for a  $\gamma \sim \mathcal{O}(1)$  Alnico spin source.

The bounds for a neutron star with the same mass of the sun traveling at  $v \sim 10^{-3}$  with respect to the ether rest frame are

$$\frac{M}{F} < \left( \frac{M}{10^5 \text{ GeV}} \right)^{5/2} \quad (\text{to be predictive}), \quad \frac{M}{F} < \left( \frac{M}{10^9 \text{ GeV}} \right)^{9/4} \quad (\text{to be linear}). \quad (54)$$

A plot of these bounds appear in Figure 8.

## References

- [1] N. Arkani-Hamed, H.-C. Cheng, M. A. Luty, and S. Mukohyama. *Ghost Condensation and a Consistent Infrared Modification of Gravity*. [hep-th/0312099](#).
- [2] N. Arkani-Hamed, P. Creminelli, S. Mukohyama, and M. Zaldarriaga. *Ghost Inflation*. [hep-th/0312100](#).
- [3] M. Peloso, and L. Sorbo. *Moving sources in a ghost condensate*. [hep-th/0404005](#)
- [4] S. L. Dubovsky. *Star tracks in the ghost condensate*. [hep-ph/0403308](#)
- [5] J. E. Moody and F. Wilczek. *New macroscopic forces?* Phys. Rev. D **30**, 130 (1984).

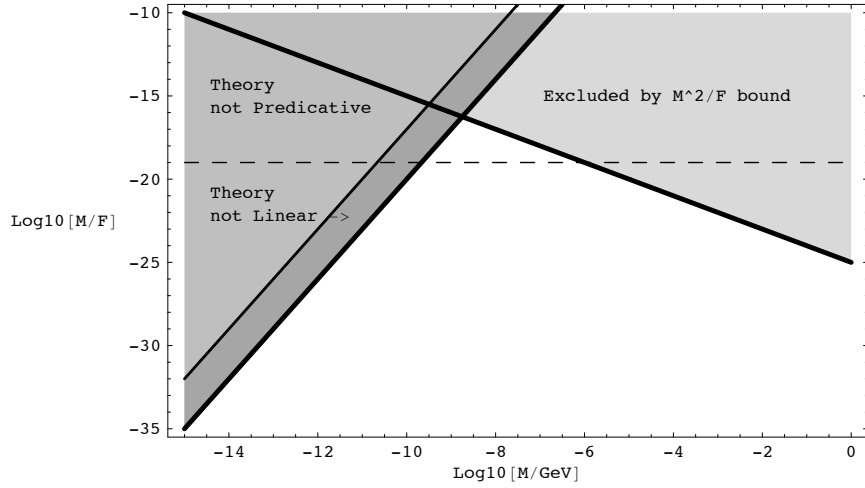


Figure 7: Bounds on the effective theory of ghostone bosons assuming an Alnico test spin of radius  $R \sim 1/Mv$ . The dashed line represents “gravitational strength,” namely the value  $M/F = (1 \text{ GeV}/M_{\text{Pl}})$  corresponding the case where the ghostone mediated force is the same strength as gravity assuming one aligned spin per nucleon.

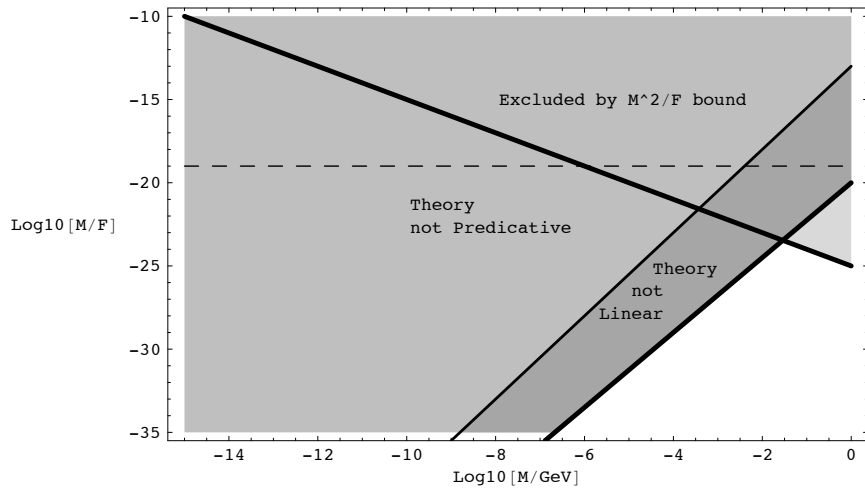


Figure 8: Bounds on the effective theory of ghostone bosons assuming a neutron star with  $S \sim 10^{56}$  and  $R \sim 1 \text{ km}$ . The dashed line represents “gravitational strength” as in Figure 7.